The Mechanism of the Zinc(II)-Zinc Amalgam Electrode Reaction in Alkaline Media As Studied by Chronocoulometric and Voltammetric Techniques

DeWitt A. Payne[1] and Allen J. Bard*

Department of Chemistry, The University of Texas at Austin, Austin, Texas 78712

ABSTRACT

The reduction of zinc(II) and the oxidation of zinc amalgam was studied in 0.18-4.0*M* KOH solutions. The primary electrochemical technique employed was potential step chronocoulometry with data acquisition on a small digital computer. The kinetic parameters were obtained by fitting the experimental charge-time curves to the complete theoretical equation for a stepwise electron transfer mechanism. The sytem was also studied by d-c and a-c polarography and linear scan voltammetry. The results of this study were compared to those of previous workers and shown to be consistent with a mechanism based on stepwise electron transfer

$$Zn(OH)_4^{2-} \rightleftarrows Zn(OH)_2 + 2\,OH^-$$

$$Zn(OH)_2 + e \rightleftarrows Zn(OH)_2^-$$

$$Zn(OH)_2^- \rightleftarrows Zn(OH) + OH^-$$

$$Zn(OH) + Hg + e \rightleftarrows Zn(Hg) + OH^-$$

One of the most significant features of the study of electrochemical kinetics during the last 20 years has been the evolution of theoretical and experimental procedures which are useful in uncovering the different stages in the complex series of processes which comprise an electrode reaction. An investigation of the kinetics of an electrochemical reaction would ideally lead to the elucidation of the nature of the various steps and a determination of their rate constants, the identification of the intermediates and products, and the determination of the adsorption isotherm for all adsorbed species. Usually, because of experimental and theoretical limitations, only part of the information is accessible for a given system. Although characterization of intermediates is of prime importance, direct observation of these may not be possible if their concentrations are too low or their lifetimes are too short. However, analysis of the current-potential relationship obtained by several nonsteady-state methods can yield further information on complex mechanisms and faster processes.

Of particular interest in this work is the study of electrode processes involving more than one electron transfer step (1). Vetter (2-4), Hurd (5), and Mohilner (6) have calculated the steady-state polarization curves for a set of two or more consecutive single electron transfer steps. Some reactions for which consecutive electron transfer mechanisms have been proposed on the basis of steady state-measurements are Tl(III)/Tl(I) (7) and quinone/hydroquinone (8). The theory of consecutive electron transfer mechanisms for electrochemical techniques involving potential steps, current steps, and a-c polarography has also been given (9-15).

The establishment of the mechanisms of an electrode reaction often requires acquiring large amounts of accurate experimental data and fitting this data to complicated theoretical equations. Digital data acquisition systems (16-21), especially those based on general purpose programmable digital computers (20, 21), have been very useful, particularly for experimental times in the sub-second region, in obtaining this data. The data obtained by these methods can be fitted to the equations in their complete form, without the necessity of approximations or linearizations sometimes required to make the analysis of data tractable. We report here a study of the zinc(II)-zinc amalgam system using several electrochemical methods and digital data acquisition techniques.

A number of studies of the alkaline zinc electrode reaction have been made. A significant part of this effort has come from the space program's search for high energy-density primary and secondary batteries and the important role of silver/zinc and zinc/air primary batteries in this connection. Although studies of the alkaline zinc electrode reaction often are concerned with reactions at the pure metal electrode, it is common practice in batteries to amalgamate the zinc plates. Hence, we deemed a study of the alkaline zinc(I)-zinc amalgam electrode reaction justified. Moreover, the reaction at the amalgam electrode is easier to understand than the reaction at the pure metal electrode, which may be complicated by the crystallization process and more difficult surface preparation.

A number of workers (22-31) have studied the alkaline zinc(II)-zinc amalgam electrode reaction with somewhat different results. Gerischer (22, 23) determined reaction orders of hydroxide, zinc, and zincate by measuring the change of the charge transfer resistance with concentration and expressed the exchange current, i_o, as

$$i_o = 2FAk^o[Zn(OH)_4^=]^{0.5}[Zn(Hg)]^{0.5}[OH^-]^{0.0} \quad [1]$$

This result led to the reaction mechanism in Eq. [2] and [3]

$$Zn(OH)_4^{2-} \overset{\text{fast}}{\rightleftarrows} Zn(OH)_2 + 2\,OH^- \quad [2]$$

$$Zn(OH)_2 + 2e \rightleftarrows Zn(Hg) + 2\,OH^- \quad [3]$$

Farr and Hampson (24) duplicated Gerischer's results in ultrapure solutions by faradaic impedance measurements. Matsuda and Ayabe (25) studied the reduction

* Electrochemical Society Active Member.
[1] Present address: Tennessee Eastman Company, Kingsport, Tennessee 37660.
Key words: potential step chronocoulometry, electrode reaction kinetics, polarography, digital data acquisition, consecutive electron transfer reactions.

process by d-c polarography and found that the mechanism was the same as that of Gerischer, but that α was 0.42 Behr *et al.* (26) and Morinaga (27) also obtained results which were consistent with the above mechanism. Stromberg and co-workers (28-31) obtained results which were similar to those of Matsuda and Ayabe (25) for the reduction process but found that the oxidation process did not fit the mechanism proposed from the study of the reduction reaction. They proposed that the reduction and the oxidation involved two different, totally irreversible reactions, each involving a single two-electron transfer step. Their mechanism for the oxidation reaction was

$$Zn(Hg) + OH^- \rightarrow Zn(OH)^+ + 2e \quad [4]$$

$$Zn(OH)^+ + 3\ OH^- \rightarrow Zn(OH)_4^{2-} \quad [5]$$

with $\alpha_R = 0.39$ (for [3]) and $1 - \alpha_O = 0.23$ (for [4]).

The measurements of Gerischer, Morinaga, and Farr and Hampson showed that there was essentially no dependence of the exchange current on hydroxide concentration, while the mechanism of Popova and Stromberg (31) would predict a fairly large variation of exchange current with hydroxide concentration. The mechanism we propose, based on the results shown below, involves consecutive one-electron transfer steps.

Experimental

Chemicals.—Stock solutions of 4.0*M* KOH and 4.0*M* KF were prepared from "Baker Analyzed" Reagent grade KOH and KF obtained from the J. T. Baker Chemical Company. The KOH solution was standardized by titrating a known amount of reagent grade potassium biphthalate using phenolphthalein as an end-point indicator. A stock solution of 0.05*M* zinc(II) was made by dissolving "Baker Analyzed" ZnO in 50 ml of stock KOH solution. The Zn(II) solution was standardized by titrating with EDTA buffered to pH 10. Purification of experimental solutions with acid washed activated charcoal (Barker's method) was tried, but the results were the same with or without this step, so this procedure was not used regularly. Solutions were prepared by pipeting a known amount of KOH stock solution into a volumetric flask and then diluting with the stock KF solution, so that all solutions were at the same ionic strength. Zinc amalgam was prepared from 99.9% zinc wire and purified mercury. The zinc wire was amalgamated by dipping in mercuric chloride solution for a few seconds before it was placed in the mercury to aid in more rapid dissolution of the zinc. The amalgam was stored under vacuum and removed from the storage vessel under a blanket of prepurified helium. Under these conditions, the concentration of zinc in the amalgam would remain stable for more than a week.

All experiments were carried out under a blanket of nitrogen. Commercial water-pumped nitrogen was purified by first bubbling it through distilled water, then through a solution of vanadous chloride standing over saturated zinc amalgam, then passing over copper strands heated to at least 350°C, and finally through distilled water again. The copper strands had previously been exposed to oxygen at high temperature and then been reduced by passage of hydrogen gas at high temperature in order to assure an active surface. The water used in all experiments and in preparation of solutions was deionized water that had been further purified by distillation from alkaline potassium permanganate in a Barnstead water still; its conductivity was less than 10^{-7} (ohm-cm)$^{-1}$. Potassium hydroxide, potassium fluoride dihydrate, and zinc oxide were reagent grade chemicals and were used without further purification. Commercial mercury was washed in 5% HNO_3 with air bubbling for several days, then splashed at least twice through a 5% HNO_3 scrubbing tower. After drying, the mercury was distilled twice under vacuum.

Apparatus.—A single compartment electrolytic cell manufactured by Metrohm Ltd. (Model EA664) and obtained from Brinkmann Instruments was used for all experiments. The working electrode was either a hanging mercury drop electrode (h.m.d.e.) or a dropping mercury electrode (d.m.e.). The auxiliary or counterelectrode was a piece of platinum wire immersed directly in the solution. The reference electrode was a saturated calomel electrode (SCE) which was separated from the solution by a Luggin-Haber capillary. The tip of the capillary was placed as close as possible to the working electrode to minimize uncompensated resistance. The hanging mercury drop electrode was manufactured by Metrohm Ltd. (Model E-410). A fresh drop of 0.032 cm^2 theoretical area was used for each run. The capillary tip had to be cut off at intervals since the strong alkali solution attacked the glass, and eventually the tip would not hold a drop of the proper size. Electrical contact to the drop was made by inserting a platinum wire into the reservoir through the pumping nipple.

The d.m.e. was constructed from a length of Sargent 6-12 second capillary. The mercury flow rate of the d.m.e. was measured before each experiment since the capillary did not last long before the tip had to be cut off, changing the flow rate.

Potential step chronocoulometry was performed with an instrument previously described (32) constructed from Philbrick solid-state operational amplifiers. A fraction of the voltage generated by the current follower could be fed back to the potentiostat for resistance compensation; the stabilization scheme of Brown *et al.* (33) was used. A-C and d-c polarography were performed using a Princeton Applied Research Corporation, Princeton, New Jersey, Model 170 electrochemical instrument. Data from potential step experiments were taken using a PDP-12A computer system (Digital Equipment Corporation, Maynard, Massachusetts). Data for potential sweep experiments at sweep rates below 300 mV/sec were recorded on a Moseley 2D-2 X-Y recorder. For sweep rates above 300 mV/sec, a Tektronix Model 564 storage oscilloscope was used with Type 2A3 (Y axis) and Type 2A63 (X-axis) plug-ins. Permanent records of oscilloscope data were made with a Polaroid camera mounted on the oscilloscope using 3000 speed film.

Initial and final potentials for potential step experiments and initial potentials for potential sweep experiments were measured with a United Systems Corporation Model 204 voltmeter to an accuracy of ± 1 mV. Two of the relays in the relay register of the PDP-12 computer were used to control the potentiostat and integrator. Timing of data acquisition was controlled by internal computer cycle counting; the time scale was calibrated by acquiring data from a function generator (Wavetek Model 114).

Data were taken at the same potentials and the same time scales with and without zinc present. Different time scales were used at different potentials so that the charge measured with zinc was significantly larger than that without zinc, but at short enough times that sufficient kinetic information was still present. The quantity $n\mathbf{F}AD^{1/2}C/\pi^{1/2}$, which is the slope of a Q *vs.* $t^{1/2}$ plot when the potential is stepped far enough so that the reaction rate is controlled by mass transfer, was evaluated for the reduction of zinc(II) by stepping from -1.0 to -1.7V and for the oxidation of zinc amalgam by stepping from -1.7 to -1.0V and least squares analysis on the $Q - t^{1/2}$ data. Three or four steps were averaged for each potential using a fresh drop each time.

The data acquisition system was checked by recording a current-time curve with a simple RC dummy cell ($R = 5$ kohm, $C = 1\ \mu f$) for the potential stepped from 0 to $+0.400$V. The accuracy of measurement was 1.2% or better. Further details about the apparatus, procedures, and calibrations are available (34).

Theory

The best method of proving that a charge transfer reaction consists of more than one electron transfer step is to demonstrate the existence of the intermediate products by some unambiguous technique (1).

Consider the case

$$O + n_1e \rightleftarrows Y \quad E_1^{o'} \qquad [6]$$

$$Y + n_2e \rightleftarrows R \quad E_2^{o'} \qquad [7]$$

At equilibrium, from the Nernst equations for [6] and [7]

$$\frac{C_Y^{n_1+n_2}}{C_R^{n_1}C_o^{n_2}} = K = \exp\left\{\frac{n_1n_2\mathbf{F}}{RT}(E_1^{o'} - E_2^{o'})\right\} \qquad [8]$$

Hence, for a given total concentration of O and R, C^*, the maximum amount of Y is present when $C_R = C_O$. If $E_1^{o'}$ is much greater than $E_2^{o'}$, then solutions containing essentially only Y can be made. If $E_1^{o'} = E_2^{o'}$, then $K = 1$ and for $n_1 = n_2 = 1$, the maximum C_Y is given by $C_O = C_Y = C_R$. As the quantity $E_1^{o'} - E_2^{o'}$ becomes more negative, the maximum amount of Y that can be present decreases rapidly. For example, for $n_1 = n_2 = 1$, and $C_O = C_R = C^*$, if $E_1^{o'} - E_2^{o'} = -0.2$V, then $C_Y \approx 0.03\ C^*$, while if $E_1^{o'} - E_2^{o'} = -0.4$V, $C_Y \approx (4 \times 10^{-4})C^*$.

However, depending upon the values of the rate constants for steps [6] and [7], the existence of stepwise electron transfer and transient formation of an intermediate, Y, can be deduced from electrochemical measurements [see Ref. (1) and general treatment of Albery and Hitchman (35)].

Potential step chronocoulometry (33, 34) was chosen as the principal electrochemical investigative procedure in this research, because integration of the current signal removes most of the high-frequency noise from this signal. Moreover, the integrated signal always starts from zero and can always be adjusted to stay on a given scale, while in chronoamperometry initial double-layer charging current may be several orders of magnitude larger than the faradaic current so that to obtain sufficient precision in the region of interest, the signal must be allowed to overdrive the amplifiers of the measuring instrument. Chronocoulometry can also be used to obtain information about the double layer (36, 37). Although the theoretical equations for stepwise electron transfers in chronocoulometry have not been presented previously, they can be obtained quite easily by integration of the appropriate equations of chronoamperometry.

Potentiostatic current-time behavior for systems involving a quasi-reversible two-step charge transfer was first derived by Hung and Smith (10) for the analytical solution for this case in a-c polarography. The partial differential equations and boundary conditions used by these authors in obtaining the following results are given in the Appendix. For the reaction given in Eq. [6] and [7] and following the notation of Hung and Smith (10), let

$$\psi_i(t) = \frac{i_1(t)}{n_i\mathbf{F}AC^*_oD_o^{1/2}} \qquad [9]$$

$$\beta_i = 1 - \alpha_i \ (i = 1,2) \qquad [10]$$

$$D_1 = D_O^{\beta_1}D_Y^{\alpha_1} \quad D_2 = D_Y^{\beta_2}D_R^{\alpha_2} \qquad [11]$$

$$f_1 = f_O^{\beta_1}f_Y^{\alpha_1} \quad f_2 = f_Y^{\beta_2}f_R^{\alpha_2} \qquad [12]$$

$$E^r_{1/2,1} = E_1^{o'} - \frac{RT}{n_1\mathbf{F}}\ln\left(\frac{f_Y}{f_O}\right)\left(\frac{D_O}{D_Y}\right)^{1/2} \qquad [13]$$

$$E^r_{1/2,2} = E_2^{o'} - \frac{RT}{n_2\mathbf{F}}\ln\left(\frac{f_R}{f_Y}\right)\left(\frac{D_Y}{D_R}\right)^{1/2} \qquad [14]$$

$$j_i = \frac{n_i\mathbf{F}}{RT}(E - E^r_{1/2,i}) \ (i = 1,2) \qquad [15]$$

These authors showed that the current during a step to potential E is given by Eq. [16].

$$i(t) = \mathbf{F}AC^*_OD_O^{1/2}[n_1\psi_1(t) + n_2\psi_2(t)] \qquad [16]$$

where

$$\psi_1(t) = \frac{\lambda_1}{(1 + e^{j_1})(\chi_+ + \chi_-)}[(\chi_- - \lambda_2)\exp(\chi_-^2t)\operatorname{erfc}(\chi_-t^{1/2}) - (\chi_+ - \lambda_2)\exp(\chi_+^2t)\operatorname{erfc}(\chi_+t^{1/2})] \qquad [17]$$

$$\psi_2(t) = \frac{\lambda_1\lambda_2}{(1 + e^{j_1})(1 + e^{j_2})(\chi_- - \chi_+)}[\exp(\chi_+^2t)\operatorname{erfc}(\chi_+t^{1/2}) - \exp(\chi_-^2t)\operatorname{erfc}(\chi_-t^{1/2})] \qquad [18]$$

$$\chi\pm = \frac{\lambda_1 + \lambda_2 \pm [(\lambda_1 + \lambda_2)^2 - 4K]^{1/2}}{2} \qquad [19]$$

$$K = \lambda_1\lambda_2\left[\frac{e^{j_2} + e^{-j_1} + e^{(j_2-j_1)}}{(1 + e^{j_2})(1 + e^{j_1})}\right] \qquad [20]$$

$$\lambda_i = \frac{k^o_if_i}{D_i^{1/2}}(e^{-\alpha_ij_i} + e^{\beta_ij_i}) \qquad (i = 1,2) \qquad [21]$$

Since we are interested here only in the case where $E_1^{o'} << E_2^{o'}$, and because $E \approx E^r_{1/2} = (E^r_{1/2,1} + E^r_{1/2,2})/2$, some simplifications can be made in these equations, yielding

$$\psi_1(t) = \frac{\lambda_1}{(1 + e^{j_1})(\lambda_1 + \lambda_2)}[\lambda_2\exp(\chi_-^2t)\operatorname{erfc}(\chi_-t^{1/2}) + \lambda_1\exp(\chi_+^2t)\operatorname{erfc}(\chi_+t^{1/2})] \qquad [22]$$

$$\psi_2(t) = \frac{\lambda_1\lambda_2}{(1 + e^{j_1})(\lambda_1 + \lambda_2)}[\exp(\chi_-^2t)\operatorname{erfc}(\chi_-t^{1/2}) - \exp(\chi_+^2t)\operatorname{erfc}(\chi_+t^{1/2})] \qquad [23]$$

The expression for $Q(t)$ is obtained by integrating the above equations to obtain Eq. [24] and [25]

$$\int\psi_1(t)\,dt = \frac{\lambda_1}{(1 + e^{j_1})(\lambda_1 + \lambda_2)}\left[\frac{\lambda_2}{\chi_-^2}\left(\exp(\chi_-^2t)\operatorname{erfc}(\chi_-t^{1/2}) + \frac{2\chi_-t^{1/2}}{\pi^{1/2}} - 1\right) + \frac{\lambda_1}{\chi_+^2}\left(\exp(\chi_+^2t)\operatorname{erfc}(\chi_+t^{1/2}) + \frac{2\chi_+t^{1/2}}{\pi^{1/2}} - 1\right)\right] \qquad [24]$$

$$\int\psi_2(t) = \frac{\lambda_1\lambda_2}{(1 + e^{j_1})(\lambda_1 + \lambda_2)}\left[\frac{1}{\chi_-^2}\left(\exp(\chi_-^2t)\operatorname{erfc}(\chi_-t^{1/2}) + \frac{2\chi_-t^{1/2}}{\pi^{1/2}} - 1\right) - \frac{1}{\chi_+^2}\left(\exp(\chi_+^2t)\operatorname{erfc}(\chi_+t^{1/2}) + \frac{2\chi_+t^{1/2}}{\pi^{1/2}} - 1\right)\right] \qquad [25]$$

Since χ_+ is much greater than χ_-, the term in the above equations in χ_+ can be neglected compared to the term in χ_-. Under these conditions, then

$$\int\psi_1(t)\,dt = \int\psi_2(t)\,dt \qquad [26]$$

and, defining Z_c as in Eq. [27]

$$Z_c = \frac{(n_1 + n_2)\mathbf{F}AD_O^{1/2}C^*_O\lambda_1\lambda_2}{(1 + e^{j_1})(\lambda_1 + \lambda_2)} \qquad [27]$$

then

$$Q(t) = \frac{Z_c}{\chi_-^2}\left(\exp(\chi_-^2t)\operatorname{erfc}(\chi_-t^{1/2}) + \frac{2\chi_-t^{1/2}}{\pi^{1/2}} - 1\right) \qquad [28]$$

For the case where R is initially present but not O and the potential is stepped in the positive direction, the expression for $Q(t)$ is the same as that in [28] except that Z_c is replaced by Z_a

$$Z_a = \frac{(n_1 + n_2)\mathbf{F}AD_R^{1/2}C^*_R\lambda_1\lambda_2}{(1 + e^{-j_2})(\lambda_1 + \lambda_2)} \quad [29]$$

Thus, for a two-step electron transfer reaction, the equation for $Q(t)$ is identical in form to the expression for $Q(t)$ for single-step charge transfer, Eq. [30] (36, 37)

$$Q(t) = \frac{K}{\lambda^2}\left(\exp(\lambda^2 t)\,\mathrm{erfc}\,(\lambda t^{1/2}) + \frac{2\lambda t^{1/2}}{\pi^{1/2}} - 1\right) \quad [30]$$

$$\lambda = \frac{k^o}{D^{1/2}}(e^{-\alpha j} + e^{\beta j}) \quad [31]$$

$$j = \frac{n\mathbf{F}}{RT}(E - E^{o\prime}) \quad [32]$$

$$K = n\mathbf{F}Ak^o(C^*_O e^{-\alpha j} - C^*_R e^{\beta j}) \quad [33]$$

To use Eq. [28] or [29] to determine kinetic parameters and reaction mechanisms, one steps from a potential where no appreciable current flows to one where a measurable cathodic or anodic current is obtained and measures the Q *vs.* t behavior. From this data K and λ are determined. These values are determined at a number of potentials and then the logarithm of K and λ are plotted *vs.* the potential. For a single-step charge transfer case, the plot of ln K *vs.* E is a straight line with a slope equal to $-\alpha n\mathbf{F}/RT$. The plot of ln λ *vs.* E is a curve which has a minimum near $E^{o\prime}$ and asymptotically approaches straight lines for E greater than and less than $E^{o\prime}$. The slope of the asymptote for E less than $E^{o\prime}$ is $-\alpha n\mathbf{F}/RT$, while for E greater than $E^{o\prime}$, it is $\beta n\mathbf{F}/RT$.

In the case of a two-step charge transfer reaction, Z and χ_- can be determined from Q *vs.* t (or i *vs.* t) data in the same manner as K and λ in a one-step reaction. However, the behavior of the plots of ln Z and ln χ_- *vs.* E can be more complex than in the one-step case. It is this difference in behavior that can sometimes allow one to demonstrate the existence of a two-step mechanism. The behavior of ln χ_- *vs.* E and ln Z *vs.* E can be illustrated by some examples:

(*i*) If k^o_1 and k^o_2 are very large, then the over-all rate of the reaction may be so fast that the reaction appears to be Nernstian. In this case, it is not possible to calculate χ_- and Z and the reaction is indistinguishable from a one-step multi-electron transfer reaction (10).

(ii) For $k^o_1 >> k^o_2$, when $(RT/\mathbf{F})\ln(k^o_2/k^o_1) < E < E^r_{1/2,2}$, then $\partial \ln Z_c/\partial E = -(1 + \alpha_2)\mathbf{F}/RT$ [see Fig. 1 (Z_c,1)] and ln χ_- has a minimum near $E = 0$ (where $E^r_{1/2,1}$ is taken as -0.2V, and $E^r_{1/2,2}$ is $+0.2$V). When $(RT/\mathbf{F})\ln(k^o_2/k^o_1) < E < O$, then $\partial \ln(\chi_-)/\partial E = -(1 + \alpha_2)\mathbf{F}/RT$ [Fig. 1 (χ_-,2)]. When $O < E < E^r_{1/2,2}$ $\partial \ln(\chi_-)/\partial E = (1 - \alpha)\mathbf{F}/RT$ [Fig.1 (χ_-,1)] and $\partial \ln Z_a/\partial E = \beta_2\mathbf{F}/RT$ [Fig. 1 (Z_a,1)]. When $E^r_{1/2,1} < E < (RT/\mathbf{F})\ln(k^o_2/k^o_1)$, then $\partial \ln Z_c/\partial E = -\alpha_1\mathbf{F}/RT$ [Fig. 1 (Z_c,2)], $\partial \ln Z/\partial E = (2 - \alpha_1)\mathbf{F}/RT$ [Fig. 1 (Z_a,2)] and $\partial \ln(\chi_-)/\partial E = -\alpha_1\mathbf{F}/RT$ [Fig. 1 (χ_-,3)].

(*iii*) For $k^o_2 >> k^o_1$, the results are the mirror image of those for case (*ii*) above.

(*iv*) The results for $k^o_2 = k^o_1$ are shown in Fig. 2. Therefore, to determine whether a reaction is single step or multi-step, not only must the over-all reaction be slow enough to be measurable, but also the rate must be slow enough to be measurable in the vicinity of

$$E' = \frac{E^r_{1/2,1} + E^r_{1/2,2}}{2} + \frac{RT}{\mathbf{F}}\ln\frac{k^o_2}{k^o_1} \quad [34]$$

Otherwise, the reaction is indistinguishable from a single-step reaction. For example, for $k^o_2 >> k^o_1$, if the most positive potential at which measurements of Z and χ_- can be made is less than E' in 38, then $\partial \ln Z_a/\partial E = (2 - \alpha_1)\mathbf{F}/RT$ and $\partial \ln Z_c/\partial E = -\alpha_1\mathbf{F}/RT$. Under these conditions $\partial \ln Z_a/\partial E - \partial \ln Z_c/\partial E = 2\mathbf{F}/RT$ and the results cannot be distinguished from a single-step reaction with the same over-all rate and $\alpha = \alpha_1/2$. The behavior of ln (χ_-) is similarly indistinguishable.

In order to assign values to both α_1 and α_2, both cathodic and anodic plots of ln Z and ln χ_- *vs.* E must have linear segments whose slope is less than $n_1\mathbf{F}/RT$.

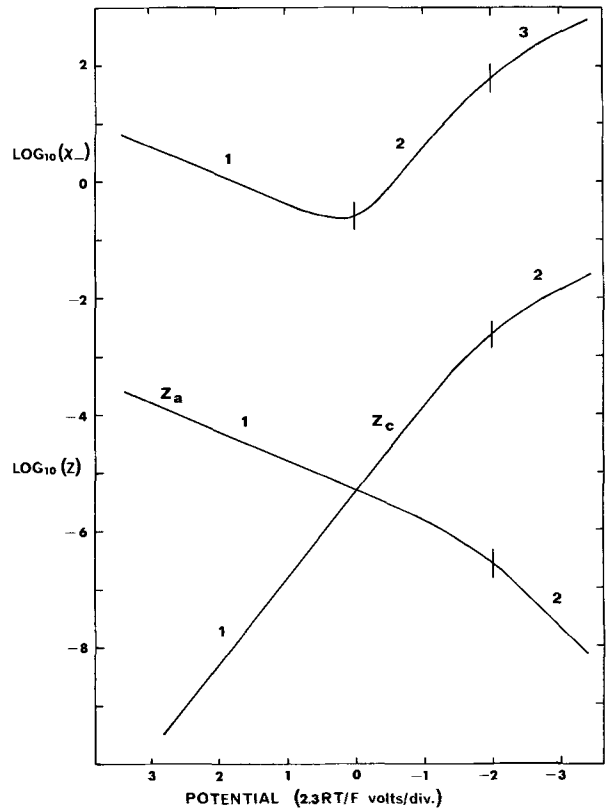

Fig. 1. Log χ_- and log Z vs. E for case (*ii*). $\alpha_1 = \alpha_2 = 0.5$, $E^r_{1/2,1} = -0.2$V, $E^r_{1/2,2} = +0.2$, $k^o_1 = 2.0$, $k^o_2 = 0.02$, $n_1 = n_2 = 1$, $D_1^{1/2} = D_2^{1/2} = 0.00316$, $f_1 = f_2 = 1.0$, $C_O = C_R = 2.03 \times 10^{-6}$ moles/cm^3, $A = 0.032$ cm^2.

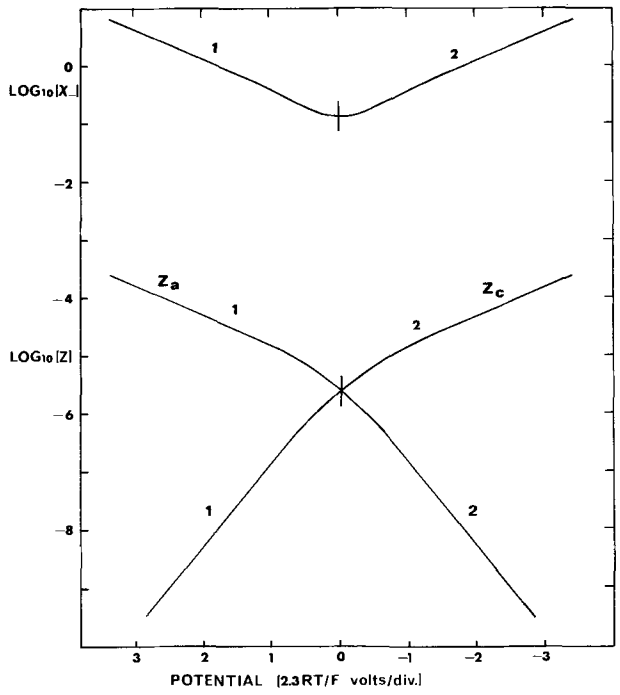

Fig. 2. Log χ_- and log Z vs. E from case (*iv*). The conditions are the same as in Fig. 1 except $k^o_1 = 0.02$.

Then α_1 can be obtained from the slope of the cathodic plot and α_2 can be obtained from the slope of the anodic plot. $(E^r_{1/2,1} + E^r_{1/2,2})/2$ can be determined from the potential where $Z_a = Z_c$

$$E_{Z_a=Z_c} = \frac{n_1 E^r_{1/2,1} + n_2 E^r_{1/2,2}}{n_1 + n_2} + \frac{RT}{(n_1 + n_2)\mathbf{F}} \ln \frac{C^*_O}{C^*_R} \quad [35]$$

Even here k^o_1, k^o_2, $E^r_{1/2,1}$, and $E^r_{1/2,2}$ cannot be assigned absolute values, since the value of $E^r_{1/2,2} - E^r_{1/2,1}$ is not known. We can, however, measure k_1' and k_2' at $(E^r_{1/2,1} + E^r_{1/2,2})/2$.

For $n_1 = n_2 = 1$

$$k_1' = \frac{k^o_1}{\exp\left[\frac{-\alpha_1 \mathbf{F}}{RT}\left(\frac{E^r_{1/2,2} - E^r_{1/2,1}}{2}\right)\right]} \quad [36]$$

$$k_2' = \frac{k^o_2}{\exp\left[\frac{(1-\alpha_2)\mathbf{F}}{RT}\left(\frac{E^r_{1/2,2} - E^r_{1/2,1}}{2}\right)\right]} \quad [37]$$

If we could measure the concentration of Y at equilibrium, we could then determine the value of $E^r_{1/2,2} - E^r_{1/2,1}$. For purposes of calculation it is sufficient to select a value of $E_2 - E_1$ greater than 0.2V and use that to calculate k^o_1 and k^o_2 from the observed k_1' and k_2'. Using the values determined above for α_1, α_2, $E^r_{1/2,1}$, $E^r_{1/2,2}$, n_1, n_2, k^o_1, and k^o_2, one can calculate Z and χ_- over the whole potential range and see if these values give a good fit in the nonlinear portions of the ln Z and ln χ_- *vs.* E plots. If the fit is good, one can say with confidence that the charge transfer is multi-step.

Clearly, potential step techniques are particularly useful for distinguishing between single-step and multi-step electron transfer. Hurd (5) has stated that unequivocal proof of a two-step consecutive electron transfer mechanism can only be obtained from steady-state polarization curves if the exchange currents of the two steps differ by a factor of 100 or more while still being less than the mass transfer limited current. Hence, if rate constants are about equal, concentration ratios would have to be very large in order to achieve the necessary exchange currents. Large concentration ratios usually mean large concentrations, high currents, and problems from solution resistance. Potential step techniques allow examination of the current-potential behavior over a wider range of potentials and larger rates than is possible with steady-state techniques since the effects of mass transfer can be accounted for by proper application of potential step theory.

Results

Potential step chronocoulometry.—Kinetic parameters are usually determined by linearization of Eq. [30] by taking Q values only at times where $\lambda t^{1/2} > 5$, so that exp $(\lambda^2 t)$ erfc $(\lambda t^{1/2})$ is negligible compared to the other terms in this equation (36). A similar procedure is often followed in chronoamperometric experiments (38, 39) where current values at times corresponding to $\lambda t^{1/2} < 0.1$ are used. The difficulty of using these approximations in practice has been discussed [see, for example (40, 41)] and is based on the necessity of knowing the value of λ, the parameter to be determined by the experiment, before the valid approximation zone is established. Moreover, the zone of the approximation may be located where perturbations caused by double layer charging or convection are important. However, the best use of the data is made by fitting the experimental results to the complete theoretical Eq. [30] using a high speed digital computer, and this procedure was followed here. Because digital data acquisition was employed, the data were in a particularly convenient form for further processing on the computer. The procedure followed consisted of guessing initial values of K and λ and calculating values of Q for each t using [30], Q_{calc}. These values are compared to the experimental ones, Q_{exp}, and the total variance, which is the sum of $(Q_{exp} - Q_{calc})^2$, determined. The values of K and λ are changed until the variance has been minimized. Details of this procedure and the method for calculating exp (y^2) erfc (y) are discussed elsewhere (34). Preliminary chronocoulometric measurements showed that neither reactant (zincate) or product (zinc in mercury) were adsorbed, so that the number of coulombs required to charge the double layer capacitance, Q_{dl}, was determined on a test solution lacking zinc(II) with a pure mercury electrode; Q_{exp} was then taken as $Q_{meas} - Q_{dl}$, where Q_{meas} is the measured charge. This procedure assumes that Q_{dl} is not affected significantly by the presence of the small amounts of zinc in solution or mercury.

The log λ and log K values at various potentials and various hydroxide concentrations determined by this procedure are given in Table I. These values were plotted *vs.* E and αn and βn were determined from the slopes of the linear parts of the cathodic and anodic branches of the plots at constant hydroxide concentration. The dependence on hydroxide ion concentration was determined from plots of log K at constant potential *vs.* log $[OH^-]$. The results are given in Table II. The diffusion coefficients of zinc(II) and Zn(Hg) were determined by measuring K/λ when $|E - E^r_{1/2}|$ was large. For the reduction process, this gives the value of $n\mathbf{F}AC^*_O D_O^{1/2}$, while for the oxidation $n\mathbf{F}AC^*_R D_R^{1/2}$. The effective surface area of the Kemula type Metrohm h.m.d.e. has been shown to be about 90% of the geometrical area (42) yielding a value for our electrode of 0.0291 cm^2. With this value for A, $C^*_O = 2.03 \times 10^{-6}$ moles/cm^3 and $K_c/\lambda = 2.82 \times 10^{-5}$, we obtain a $D_O^{1/2} = 2.47 \times 10^{-3}$ cm/sec$^{1/2}$. Similarly, with $K_a/\lambda = 2.66 \times 10^{-5}$ and $D_R^{1/2} = 3.98 \times 10^{-3}$ cm/sec$^{1/2}$ (43), the concentration of zinc in the amalgam, C^*_R, was found to be 1.19 mM. The potentials for the intersection of K_a and K_c and the concentrations of Zn(II) Zn(Hg), and OH^- can be used to calculate $E^r_{1/2}$ for the over-all reaction. A plot of $E^r_{1/2}$ *vs.* log $[OH^-]$ had a slope of -0.118V and an intercept of -1.445V *vs.* SCE.

D-C polarography.—The zinc(II)/zinc amalgam system in alkaline media exhibits a quasi-reversible polarographic reduction wave. The treatment of the data follows the treatment of Meites and Israel (44) and is similar to that of Matsuda and Ayabe (25). From the Ilkovic equation and the values $m = 1.07$ mg/sec, $t = 1.0$ sec, $i_d = 7.64$ μA and $C^*_O = 2.03$ mM, we find a value of $D_O^{1/2} = 2.53 \times 10^{-3}$ cm/sec$^{1/2}$, in good agreement with the value obtained from the potential step experiment. To determine kinetic data, a plot of $\log[i/(i_d - i)]$ *vs.* E according to the equation for a totally irreversible reaction (44)

$$E = E^{o'} + \frac{0.059}{\alpha n} \log \frac{1.349 k^o t^{1/2}}{D_O^{1/2}} - \frac{0.0542}{\alpha n} \log \frac{i}{i_d - i} \quad [38]$$

was made for values of E sufficiently negative as to make the reverse reaction slow enough to be negligible. Results are given in Table II.

A-C polarography.—Measurement of kinetic parameters by a-c polarography involved phase-sensitive detection of the current, so that the phase angle of the current as well as its magnitude was measured. From this data the cotangent of the phase angle, θ, was determined and used to calculate λ at different values of E (45)

$$\text{Cot}\,(\theta) = I_{0^\circ}/I_{90^\circ} = 1 + (2\omega)^{1/2}/\lambda \quad [39]$$

The kinetic parameters can be obtained from a plot of log λ *vs.* E or directly from a plot of cot (θ) *vs.* E by measuring the potential and magnitude of the maximum value of cot (θ) (45)

Table I. Potential step chronocoulometry. Results

(a) Reduction reaction; Steps from −1.00V *vs.* SCE to *E*; solution contained 2.03 m*M* zinc(II) and KOH; electrode was Hg drop

[OH⁻]	*E* (V *vs.* SCE)	Log λ	Log *K*	Stand. dev. × 10⁹
0.18	−1.36	−0.5675	−5.4399	6.74
	−1.38	−0.3189	−5.0049	9.12
	−1.40	+0.0055	−4.6406	11.20
	−1.42	0.3193	−4.3096	25.20
	−1.44	0.7663	−3.9789	25.60
	−1.46	0.7729	−3.8012	5.14
	−1.48	1.0177	−3.5614	2.46
	−1.50	1.2498	−3.3153	15.40
	−1.52	1.4933	−3.1080	13.50
0.34	−1.40	−0.6829	−5.3471	12.70
	−1.42	−0.4776	−5.0082	38.00
	−1.44	−0.1598	−4.6555	17.10
	−1.46	+0.1881	−4.3466	7.64
	−1.48	0.4876	−4.0607	6.94
	−1.50	0.8026	−3.7670	7.84
	−1.52	1.0215	−3.5505	14.40
	−1.54	1.2627	−3.3110	3.05
	−1.56	1.4239	−3.1461	2.65
0.96	−1.43	−0.5593	−5.8622	6.30
	−1.45	−0.6991	−5.4614	9.96
	−1.47	−0.4673	−5.0589	12.20
	−1.49	−0.1595	−4.7091	10.90
	−1.51	+0.1403	−4.3978	6.51
	−1.53	0.4478	−4.1129	9.58
	−1.55	0.7000	−3.8504	10.00
	−1.57	0.9316	−3.6158	2.88
	−1.59	1.1671	−3.3903	2.05
	−1.61	1.3156	−3.2317	2.02
1.76	−1.46	−0.5434	−5.8832	8.95
	−1.48	−0.6788	−5.4323	9.77
	−1.50	−0.4698	−5.0280	16.30
	−1.52	−0.1748	−4.7138	16.20
	−1.54	+0.0987	−4.4254	13.40
	−1.56	0.3821	−4.1427	11.50
	−1.58	0.6573	−3.8857	19.80
	−1.60	0.9402	−3.6369	14.50
	−1.62	1.0412	−3.4839	7.25
	−1.64	1.2536	−3.3069	7.29

(b) Oxidation reaction: Steps from −1.700V *vs.* SCE to *E*, solution contained no zinc(II) and KOH, electrode was zinc amalgam with a [Zn] = 1.2 m*M*

[OH⁻] (*M*)	*E* (V *vs.* SCE)	Log λ	Log *K*	Stand. dev. × 10⁹
0.18	−1.38	−0.2117	−5.8534	4.97
	−1.36	−0.3641	−5.4843	10.20
	−1.32	−0.4563	−5.1238	6.47
	−1.28	−0.1335	−4.7542	6.79
	−1.24	+0.1061	−4.4880	4.80
	−1.20	0.3460	−4.2348	3.65
	−1.16	0.6573	−3.9680	16.30
	−1.12	0.7993	−3.7641	2.42
	−1.08	1.0502	−3.5123	10.40
	−1.04	1.5222	−3.0975	36.40
0.34	−1.42	−0.8242	−6.0244	10.60
	−1.40	−0.8504	−5.6479	15.60
	−1.36	−0.8181	−5.1592	27.90
	−1.32	−0.1515	−4.7376	58.30
	−1.28	−0.0120	−4.4963	10.30
	−1.24	+0.3497	−4.2217	3.85
	−1.20	0.6166	−3.9595	3.45
	−1.16	0.8588	−3.7272	3.88
	−1.12	0.9097	−3.6416	8.35
	−1.08	1.2846	−3.2853	2.79
0.96	−1.47	−0.3670	−5.8545	2.77
	−1.45	−0.5167	−5.5910	4.45
	−1.41	−0.3864	−5.0590	4.33
	−1.37	−0.0143	−4.6425	12.60
	−1.33	+0.2119	−4.3768	5.53
	−1.29	0.4428	−4.1431	4.30
	−1.25	0.6871	−3.8975	2.67
	−1.21	0.8744	−3.7023	3.59
	−1.17	1.0797	−3.4987	16.00
	−1.13	1.3458	−3.2434	2.64

$$[E]_{max} = E^{r}_{1/2} + \frac{RT}{n\mathbf{F}} \ln(\alpha/\beta) \quad [40]$$

$$[\cot(\theta)]_{max} = 1 + \frac{(2\omega D)^{1/2}}{k^{o}[(\alpha/\beta)^{-\alpha} + (\alpha/\beta)^{\beta}]} \quad [41]$$

The results are shown in Table II.

Potential sweep voltammetry.—Kinetic parameters can be obtained from linear potential sweep voltammetry at a stationary electrode by observing the variation of E_p or of $E_p - E_{p/2}$ with scan rate, v (46). Kinetic parameters for the cathode reaction were obtained from experiments in a 1.0*M* KOH solution containing 2.03 m*M* zinc(II) at a mercury electrode while those for the anodic reaction used a zinc amalgam electrode, [Zn] = 1.2 m*M* and 1.0*M* KOH (34). Kinetic parameters obtained from these measurements are shown in Table II.

Discussion

The results obtained by the different electrochemical methods in Table II are in fair agreement with each other. These results show that the electrode reaction of zinc in alkaline media is not a simple quasi-reversible two-electron transfer. First, the quantity $\alpha n + \beta n$ is much less than two, when α and β are calculated from the appropriate slopes measures well away from $E^{r}_{1/2}$. Second, the log *K vs. E* plots show definite curvature in the region near $E^{r}_{1/2}$. This curvature cannot be due to double-layer effects, since the rate of change of potential at the outer Helmholtz plane with electrode potential is nearly constant in the region of interest, which is far negative of the potential of zero charge, and the solution has a high ionic strength. Nor can it be explained by uncompensated resistance, since the region of maximum curvature is in the region where *K* was less than 100 μA, and the uncompensated resistance was less than 10 ohms, *i.e.*, where the curvature was most pronounced, contributions from *IR* effects were at a minimum. These features correspond quite closely to a consecutive electron transfer mechanism, however, and the following mechanism appears to fit the experimental data quite well

$$Zn(OH)_4^{2-} \rightleftarrows Zn(OH)_2 + 2\,OH^- \quad [42]$$

$$Zn(OH)_2 + e \rightleftarrows Zn(OH)_2^- \quad [43]$$

$$Zn(OH)_2^- \rightleftarrows Zn(OH) + OH^- \quad [44]$$

$$Hg + Zn(OH) + e \rightleftarrows Zn(Hg) + OH^- \quad [45]$$

Comparison of this model to the experimental results is simplified by using a modification of the notation of Hung and Smith (10), with *O* representing $Zn(OH)_2$; *YO*, $Zn(OH)_2^-$; *YR*, Zn(OH); and *R*, Zn(Hg). With $f_o = [OH^-]^2$, $f_{YO} = 1.0$, $f_{YR} = [OH^-]^{-1}$, and $f_R = [OH^-]$, the following equations hold for $E^{r}_{1/2,1}$ and $E^{r}_{1/2,2}$

$$E^{r}_{1/2,1} = E_1^{o'} + \frac{RT}{2\mathbf{F}} \ln \frac{D_O}{D_{YO}} + \frac{RT}{\mathbf{F}} \ln \frac{f_O}{f_{YO}} \quad [46]$$

$$E^{r}_{1/2,1} = E_1^{o'} + \frac{RT}{2\mathbf{F}} \ln \frac{D_O}{D_{YO}} - \frac{RT}{\mathbf{F}} \ln[OH^-]^2 \quad [47]$$

$$E^{r}_{1/2,2} = E_2^{o'} + \frac{RT}{2\mathbf{F}} \ln \frac{D_{YR}}{D_R} - \frac{RT}{\mathbf{F}} \ln[OH^-]^2 \quad [48]$$

At constant $E - E^{r}_{1/2}$, the hydroxide dependence of λ_1 is proportional to f_1 and λ_2 to f_2, where f_1 and f_2 are given by Eq. [49] and [50]

$$f_1 = f_o^{\beta_1} f_{YO}^{\alpha_1} = [OH^-]^{-0.36} \quad [49]$$

$$f_2 = [OH^-]^{-0.32} \quad [50]$$

Table II. Summary of experimental results by different techniques

	αn	βn	$k^{o}_c/D_O^{1/2}$	$k^{o}_a/D_R^{1/2}$	$E^{r}_{1/2}$ (V *vs.* SCE)	$D_O^{1/2}$ (cm/sec$^{1/2}$)	$\frac{\partial \log K_c}{\partial \log [OH^-]}$	$\frac{\partial \log K_a}{\partial \log [OH^-]}$
Potential step	0.82	0.34	0.17	0.30	−1.445	2.47×10^{-3}	−1.85	+0.83
D-C polarography	0.82	—	0.33	—	−1.445	2.53×10^{-3}	—	—
A-C polarography	0.83	—	0.18	—	—	—	—	—
Linear potential sweep voltammetry								
(a) (E_p *vs.* log v)	0.78	0.33	0.40	0.34	—	—	—	—
(b) ($E_p - E_{p/2}$)	1.00	0.46	—	—	—	—	—	—

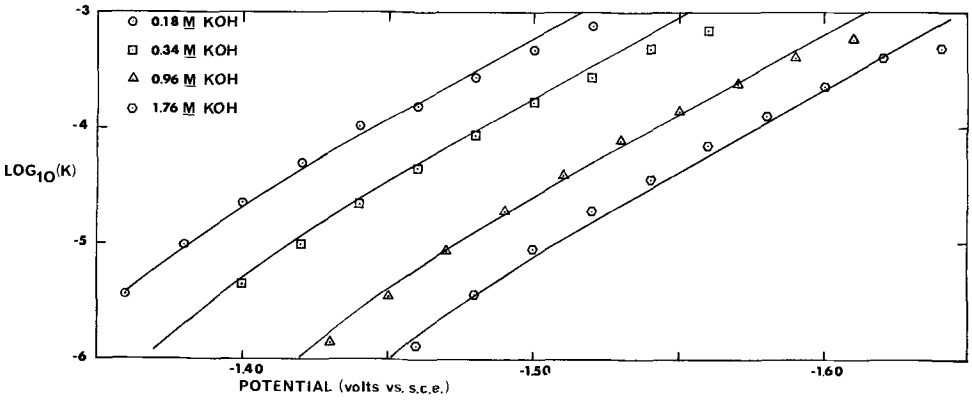

Fig. 3. Log K_c vs. E for reduction reaction. Comparison of experimental data from potential-step chronocoulometry ($[Zn(OH)_4^{2-}] = 2.03$ mM) with values calculated from consecutive-electron transfer theory.

This means that for any given value of $E - E^r_{1/2}$, the hydroxide dependence will be small. In particular, when λ_1 is nearly equal to λ_2, and the hydroxide concentration is about 1.0M, the hydroxide dependence of log K and log λ will be zero. Since the region where λ_1 is equal to λ_2 is also the region of curvature of the log K vs. E plot, the apparent α measured in this region will be between the values for the high and low slope linear regions; for the Zn(II)/Zn(Hg) reaction αn would be equal to about 1.0 in this region.

The measured values of the hydroxide dependence of log K at constant potential yield the following values for f_1 and f_2: $f_1 = [OH^-]^{-0.21}$ and $f_2 = [OH^-]^{+0.15}$. To obtain a quantitative comparison between model and results, we take $\alpha_1 = 0.82$, $\alpha_2 = 0.66$, $k^o_1 = 0.228$, $k^o_2 = 0.0209$, and use these parameters to calculate values for log K and log λ from consecutive electron transfer theory

$$E^r_{1/2,1} = -1.645 - \frac{RT}{F}\ln[OH^-]^2 \qquad [51]$$

$$E^r_{1/2,2} = -1.245 - \frac{RT}{F}\ln[OH^-]^2 \qquad [52]$$

We find that the potential step data fits the theoretical curves quite well (Fig. 3-6). In particular, in the plot of log K_a vs. E where the curvature is most pronounced, the fit is excellent.

These same parameters can also be used to calculate a-c and d-c polarograms using Hung and Smith's equations (10). In calculating polarograms, the Matsuda function (47) was used instead of exp ($\lambda^2 t$) erfc ($\lambda t^{1/2}$), because a d.m.e. is used for polarography and planar diffusion no longer occurs. The fit between the theoretical a-c polarographic data (cot θ vs. E) and d-c polarographic data [log$(i/i_d - i)$ vs. E] and the experimental results are shown in Fig. 7 and 8. The agreement between theory and experiment for a-c polarography is not too good, but Delmastro and Smith (48) pointed out that amalgam formation reactions may show large distortions of the current because of spherical diffusion inside the drop. Since the theoretical curves in these figures were calculated with parameters from the potential step experiment, the agreement must be considered satisfactory.

It is of interest to compare our results with those of previous studies (Table III). Gerischer (22, 23) and later Farr and Hampson (24) determined the exchange current i_o by measuring the charge transfer resistance ($R_T = RT/nFi_o$) at the equilibrium potential of a solution and thus determining the variation of i_o with reactant concentration. From i_o, one can determine α and k^o from the relation

$$i_o = nFAk^oC_O^{1-\alpha}C_R^{\alpha} \qquad [53]$$

The exchange current can also be determined from consecutive electron transfer theory, either from the equation derived by Vetter (2-4) or from the treatment of Hung and Smith (10)

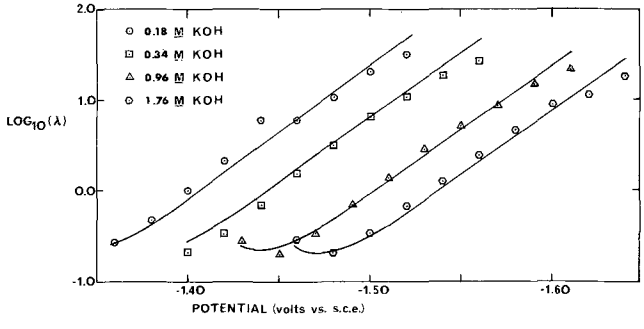

Fig. 5. Log λ vs. E for reduction reaction. Comparison of data from potential-step chronocoulometry with theoretical calculations.

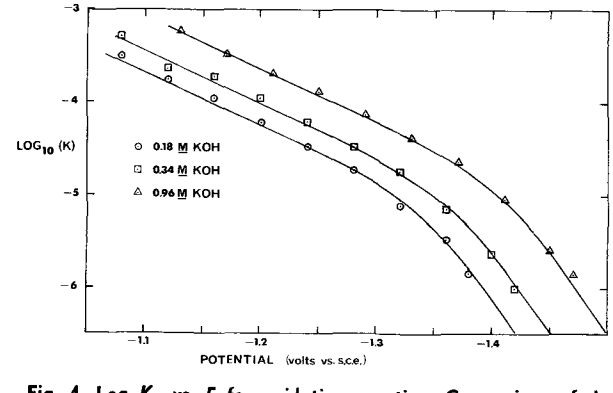

Fig. 4. Log K_a vs. E for oxidation reaction. Comparison of data from potential-step chronocoulometry ($[Zn(Hg)] = 1.2$ mM) with theoretical calculations.

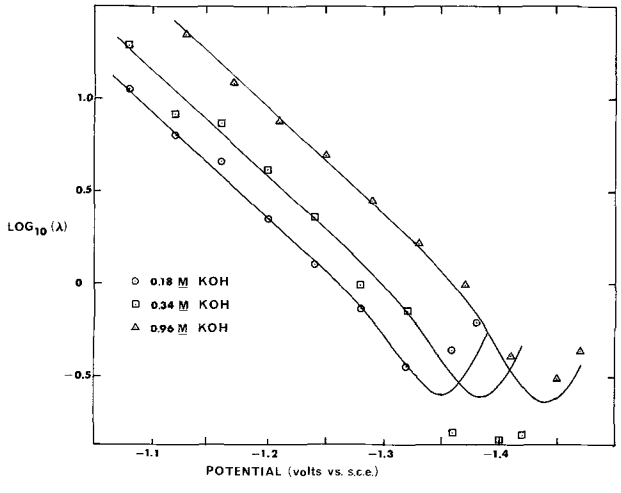

Fig. 6. Log λ vs. E for oxidation reaction. Comparison of data from potential step chronocoulometry with theoretical calculations.

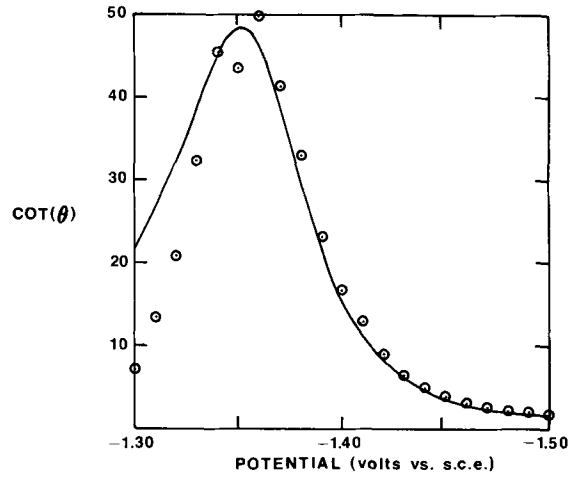

Fig. 7. Comparison of Cot(θ) vs. E data from a-c polarographic measurements with theoretical calculations. The solution contained $[Zn(OH)_4^{2-}] = 2.03$ mM and $[OH^-] = 0.18M$. The d.m.e. was mercury with a drop time of 1 sec. $\omega = 11.0$ Hz.

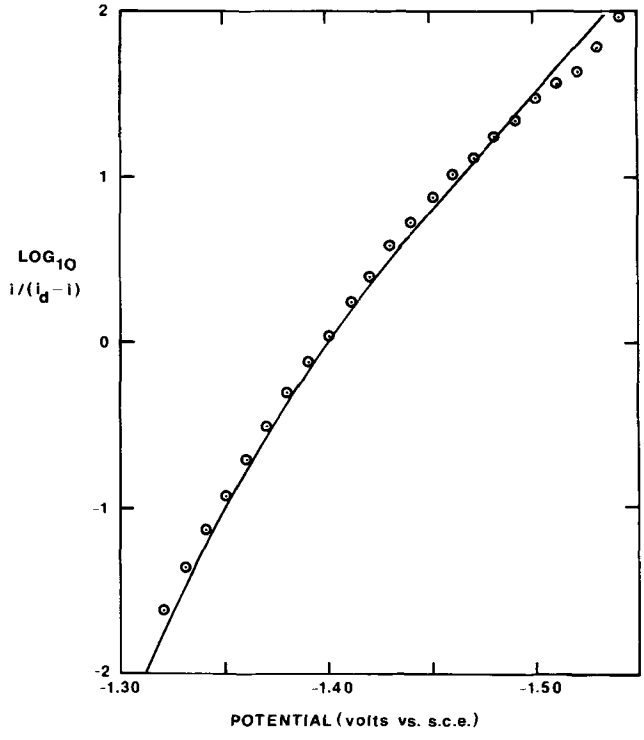

Fig. 8. Comparison of log $i/(i_d - i)$ vs. E data from d-c polarography with theoretical calculations. Conditions same as in Fig. 7.

$$i_o = 2FAC^*_O D_O^{1/2} \frac{\lambda_1\lambda_2}{(1 + e^{j_1})(\lambda_1 + \lambda_2)}$$

$$= 2FAC^*_R D_R^{1/2} \frac{\lambda_1\lambda_2}{(1 + e^{-j_2})(\lambda_1 + \lambda_2)} \quad [54]$$

Using the kinetic parameters obtained from potential step measurements to calculate i_o and R_T and comparing these results with the data in Fig. 2 of Farr and Hampson (24), we calculate an R_T which is larger than their values by a factor of 3.5. This difference may be attributed to differences in the conditions of measurement in the two studies; for example, the ionic strength of Farr and Hampson's solutions was 3.0M, while in the present work, it was 4.0M. They used NaOH and $NaClO_4$ while KOH and KF were used in the present work, and the solutions used by Farr and Hampson were purified by circulation over activated charcoal for at least 28 days. However, when the R_T values calculated from potential step data are divided by 3.5, the values at different Zn(Hg) and OH^- concentrations agree fairly well with those of Farr and Hampson (Fig. 9).

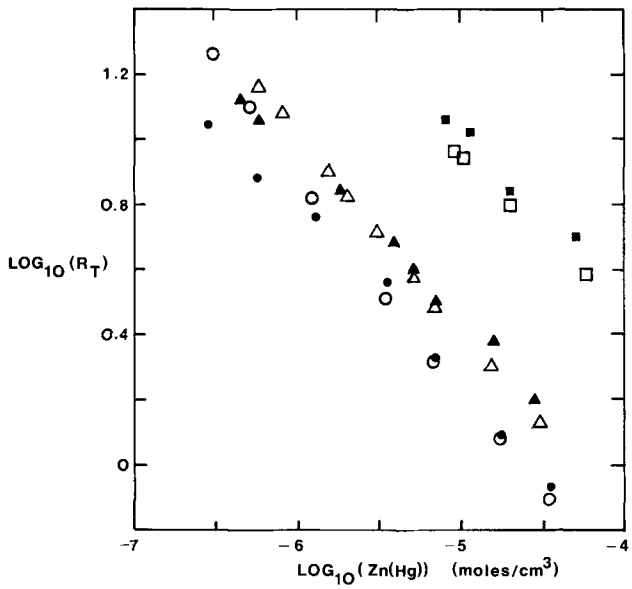

Fig. 9. Log R_T vs. log [Zn(Hg)] for different concentrations of $Zn(OH)_4^{2-}$. Comparison of theoretical calculations with experimental data from Farr and Hampson (24). Squares, $[Zn(OH)_4^{2-}] = 5.05 \times 10^{-6}$ moles/cm^3; triangles, $[Zn(OH)_4^{2-}] = 6.8 \times 10^{-5}$ moles/cm^3; circles, $[Zn(OH)_4^{2-}] = 1.834 \times 10^{-4}$ moles/cm^3. Open symbols are data from this work, solid symbols are from Farr and Hampson.

Matsuda and Ayabe (25) studied the reduction process by d-c polarography. Using the treatment for quasi-reversible polarographic waves they obtained the results shown in Table III, which agree very well with ours for the reduction process.

Stromberg and Popova (29-31) studied both the oxidation and reduction reactions by d-c polarography with a dropping zinc amalgam electrode used to study the oxidation reaction. Their results do not agree very well with the results of the present work for the oxidation reaction, although the agreement is fairly good for the reduction reaction (Table III). However, their results still lead to the conclusion that one hydroxide is involved in the oxidation reaction rate limiting step, since the oxidation rate shows a dependence on the first power of the hydroxide concentration. This observation led Stromberg and Popova to conclude that the oxidation reaction was a two-electron reaction which occurred by a completely different path than that of the reduction reaction (Eq. [4] and [5]). However, if they were correct, then a plot of log K vs. E for any one

Table III. Comparison of our results to previous studies

	αn	βn	log k^o_c	log k^o_a	$E^r_{1/2}$	$\frac{\partial \log K_c}{\partial \log [OH^-]}$	$\frac{\partial \log K_a}{\partial \log [OH^-]}$
Present work	0.82	0.34	−3.37	−2.92	−1.445	−1.85	+0.83
Farr and Hampson (24)	1.00	1.00	−3.00	—	—	—	—
Matsuda and Ayabe (25)	0.84	—	−3.3	—	−1.444	−1.82	—
Popova and Stromberg (31)	0.78	0.46	−3.43	−3.70	−1.434	−2.3	+1.4

hydroxide concentration should be linear over the whole potential range (except for curvature due to double layer effects and distortion due to uncompensated resistance); this is not the case. Moreover, this mechanism does not predict the negligible variation of the exchange current with hydroxide concentration at equilibrium which several other researchers have reported (22-24, 26, 27). The consecutive electron transfer mechanism explains all the observed features.

Recently Despic and co-workers (49) demonstrated that the Cd(II)/Cd(Hg) system in H_2SO_4 solutions, long thought to represent a mechanism involving a simple two-electron charge transfer step, probably occurs by a two-step single electron exchange mechanism. The findings here on the Zn(II)/Zn(Hg) system parallel these results and suggest that other electrode reaction mechanisms previously thought to involve multiple electron transfer steps bear reinvestigation.

Acknowledgment

The support of the National Science Foundation (NSF GP 6688X) and Delco-Remy Corporation (under AF 33(615)-3487) is gratefully acknowledged. The PDP-12A computer was acquired under a grant from the National Science Foundation (GP 10360).

Manuscript submitted April 21, 1972; revised manuscript received June 1, 1972.

Any discussion of this paper will appear in a Discussion Section to be published in the June 1973 JOURNAL.

LIST OF SYMBOLS

A	electrode area
C^*_j	bulk concentration of jth species
D_j	diffusion coefficient of jth species
f_j	activity coefficient of jth species
E^o_i	formal redox potential of ith step ($i = 1, 2$)
$E^r_{1/2,i}$	reversible half-wave potentials of ith steps
n_i	number of electrons transferred in ith charge transfer step
α_i	charge transfer coefficient for ith steps
β_i	$= 1 - \alpha_i$
k^o_i	standard heterogeneous rate constants for ith step
$\mathbf{F}$	Faraday's constant
R	ideal gas constant
T	absolute temperature
t	time
$j, \psi, \chi, \lambda, K$	derived parameters, see Eq. [15]-[21]
Z_a, Z_c	derived parameter, see Eq. [27] and [29]
$Q(t)$	charge
$i(t)$	current

APPENDIX

The equations and boundary conditions for the solution of the current-time behavior for a quasi-reversible two-step charge transfer are as follows (10)

$$\frac{\partial C_o}{\partial t} = D_o \frac{\partial^2 C_o}{\partial x^2} \quad [1A]$$

$$\frac{\partial C_Y}{\partial t} = D_Y \frac{\partial^2 C_Y}{\partial x^2} \quad [2A]$$

$$\frac{\partial C_R}{\partial t} = D_R \frac{\partial^2 C_R}{\partial x^2} \quad [3A]$$

For $t = 0$, any x

$$C_o = C^*_o \quad [4A]$$

$$C_R = C_Y = 0 \quad [5A]$$

For $t > 0$, $x \to \infty$

$$C_o \to C^*_o \quad [6A]$$

$$C_R \to C_Y \to 0 \quad [7A]$$

For $t > 0$, $x = 0$

$$D_o \frac{\partial C_o}{\partial x} = \frac{i_1(t)}{n_1 \mathbf{F} A} \quad [8A]$$

$$D_Y \frac{\partial C_Y}{\partial x} = \frac{i_2(t)}{n_2 \mathbf{F} A} - \frac{i_1(t)}{n_1 \mathbf{F} A} \quad [9A]$$

$$D_R \frac{\partial C_R}{\partial x} = \frac{-i_2(t)}{n_2 \mathbf{F} A} \quad [10A]$$

$$\frac{i_1(t)}{n_1 \mathbf{F} A k_{s,1}} = C_{o x=0} \exp\left\{\frac{-\alpha_1 n_1 \mathbf{F}}{RT}[E(t) - E_1^o]\right\} - C_{Y x=0} \exp\left\{\frac{(1-\alpha_1) n_1 \mathbf{F}}{RT}[E(t) - E_1^o]\right\} \quad [11A]$$

$$\frac{i_2(t)}{n_2 \mathbf{F} A k_{s,2}} = C_{Y x=0} \exp\left\{\frac{-\alpha_2 n_2 \mathbf{F}}{RT}[E(t) - E_2^o]\right\} - C_{R x=0} \exp\left\{\frac{(1-\alpha_2) n_2 \mathbf{F}}{RT}[E(t) - E_2^o]\right\} \quad [12A]$$

REFERENCES

1. A. Bewick and H. R. Thirsk, in "Modern Aspects of Electrochemistry," Vol. 5, p. 291ff, J. O'M. Bockris and B. E. Conway, Editors, Butterworths, Washington (1969).
2. K. J. Vetter, *Z. Naturforsch.*, **7a**, 328 (1952).
3. K. J. Vetter, *ibid.*, **8a**, 823 (1953).
4. K. J. Vetter, "Electrochemical Kinetics," p. 149ff, Academic Press, New York (1967).
5. R. M. Hurd, *This Journal*, **109**, 327 (1962).
6. D. M. Mohilner, *J. Phys. Chem.*, **68**, 623 (1964).
7. K. J. Vetter and G. Thiemke, *Z. Elektrochem.*, **64**, 805 (1960).
8. K. J. Vetter, *ibid.*, **56**, 797 (1952).
9. J. M. Hale, *J. Electroanal. Chem.*, **8**, 181 (1964).
10. H. L. Hung and D. E. Smith, *ibid.*, **11**, 237 and 425 (1966).
11. J. Plonski, *This Journal*, **116**, 1688 (1969).
12. T. Berzins and P. Delahay, *J. Am. Chem. Soc.*, **75**, 5716 (1953).
13. M. Smutek, *Coll. Czech. Chem. Comm.*, **18**, 171 (1953).
14. J. Cizek and K. Holub, *ibid.*, **31**, 689 (1966).
15. J. G. Mason, *J. Electroanal. Chem.*, **11**, 462 (1966).
16. E. R. Brown, D. E. Smith, and D. D. DeFord, *Anal. Chem.*, **38**, 1130 (1966).
17. G. Lauer and R. A. Osteryoung, *ibid.*, **38**, 1137 (1966).
18. G. L. Booman, *ibid.*, **38**, 1144 (1966).
19. M. W. Breiter, *This Journal*, **112**, 845 (1965).
20. G. Lauer, R. Abel, and F. C. Anson, *Anal. Chem.*, **39**, 765 (1967).
21. G. Lauer and R. A. Osteryoung, *ibid.*, **40**, 30A (1968).
22. H. Gerischer, *Z. Physik. Chem. (Leipzig)*, **202**, 302 (1953).
23. H. Gerischer, *Anal. Chem.*, **31**, 33 (1959).
24. J. P. G. Farr and N. A. Hampson, *J. Electroanal. Chem.*, **18**, 407 (1968).
25. H. Matsuda and Y. Ayabe, *Z. Elektrochem.*, **63**, 1164 (1959).
26. B. Behr, J. Dojlido, and J. Malyszko, *Roczniki Chem.*, **36**, 725 (1962).
27. K. Morinaga, *J. Chem. Soc. Japan*, **79**, 204 (1958).
28. A. G. Stromberg and L. F. Trushina, *Elektrokhimiya*, **2**, 1363 (1966).
29. A. G. Stromberg and L. N. Popova, *Isv. Tomsk Politekhn. Inst.*, **167**, 91 (1967).
30. A. G. Stromberg and L. N. Popova, *Elektrokhimiya*, **4**, 39 (1968).
31. A. G. Stromberg and L. N. Popova, *ibid.*, **4**, 1147 (1968).
32. F. C. Anson and D. A. Payne, *J. Electroanal. Chem.*, **13**, 35 (1967).
33. E. R. Brown, D. E. Smith, and G. L. Booman, *Anal. Chem.*, **40**, 1141 (1968).
34. D. A. Payne, Ph.D. dissertation, The University of Texas at Austin (1970).
35. J. Albery and M. Hitchman, "Ring-Disc Electrodes," pp. 38-41, Oxford University Press (1971).
36. J. H. Christie, G. Lauer, and R. A. Osteryoung, *J. Electroanal. Chem.*, **7**, 60 (1964).
37. J. H. Christie, G. Lauer, R. A. Osteryoung, and F. C. Anson, *Anal. Chem.*, **35**, 1979 (1963).
38. H. Gerischer and W. Vielstich, *Z. Physik. Chem. (Frankfurt)*, **3**, 16 (1955).

39. H. Gerischer and W. Vielstich, *ibid.*, **4**, 10 (1955).
40. K. B. Oldham and R. A. Osteryoung, *J. Electroanal. Chem.*, **11**, 397 (1966).
41. J. Osteryoung and R. A. Osteryoung, *Electrochim. Acta*, **16**, 525 (1971).
42. Katsumi Kanzaki Niki, Ph.D. dissertation, pp. 16 and 80, The University of Texas at Austin (1966).
43. A. G. Stromberg and E. A. Zakharova, *Elektrokhimiya*, **1**, 1036 (1965).
44. L. Meites and Y. Israel, *J. Am. Chem. Soc.*, **83**, 4903 (1961).
45. D. E. Smith in "Electroanalytical Chemistry," Vol. 1, p. 26ff, A. J. Bard, Editor, Marcel Dekker, New York (1966).
46. R. S. Nicholson and I. Shain, *Anal. Chem.*, **36**, 766 (1964).
47. H. Matsuda, *Z. Elektrochem.*, **59**, 494 (1955).
48. J. R. Delmastro and D. E. Smith, *Anal. Chem.*, **38**, 169 (1966).
49. A. R. Despic', D. R. Jovanovic', and S. P. Bingulac, *Electrochim. Acta*, **15**, 459 (1970).

The Kinetics of the p-Toluquinhydrone Electrode

F. Kornfeil*

Electronics Technology and Devices Laboratory,
United States Army Electronics Command, Fort Monmouth, New Jersey 07703

ABSTRACT

The reaction mechanism of the redox system p-toluquinone/toluhydroquinone (toluquinhydrone electrode) on smooth platinum was elucidated with the aid of the electrochemical reaction order method. It was found that in the *p*H range 0.1-3.2 the reaction proceeds according to the scheme $Q + H^+ \rightleftarrows HQ^+$, $HQ^+ + e^- \rightleftarrows HQ$, $HQ + H^+ \rightleftarrows H_2Q^+$, $H_2Q^+ + e^- \rightleftarrows H_2Q$. This mechanism is identical with the HeHe sequence determined by Vetter for the benzoquinone electrode. The relatively fast rate of the charge-transfer steps, however, necessitated measurements of the electrode polarization in the nonsteady state. A method is described to determine the individual exchange current densities in moderately fast consecutive charge-transfer reactions.

The reaction mechanism of the redox couple p-benzoquinone/hydroquinone (quinhydrone electrode) was first elucidated by Vetter (1) who interpreted the steady-state overpotential on smooth platinum with the aid of the electrochemical reaction order method. He showed that, in the over-all electrode reaction $H_2Q \rightleftarrows Q + 2H^+ + 2e^-$, the electrons are exchanged in two different charge-transfer steps. Hale and Parsons (2), using the Koutecky method on dropping mercury, and Eggins and Chambers (3), employing cyclic voltammetry on polished platinum electrodes, arrived at essentially similar conclusions in more recent studies of the reduction of benzoquinone and other p-quinones. The consecutive charge-transfer mechanism is, however, challenged by Loshkarev and Tomilov who account for their experimental results obtained on Pt (4, 5) and other metals (6) by postulating that both electrons are transferred simultaneously in a single charge-transfer step.

The present paper describes an investigation of the kinetics of the redox system methyl-p-benzoquinone/methyl-hydroquinone (toluquinhydrone electrode). The aim of this study has been (*i*) to clarify the situation with respect to the reaction mechanism and (*ii*) to ascertain what effect, if any, the addition of the CH_3-group to the benzene ring may have on the kinetic parameters of the quinhydrone electrode reaction.

Experimental Procedure

All measurements of the overpotential were made at the same constant temperature (25° ± 0.5°C) in solutions of equal ionic strength $\frac{1}{2}\Sigma c_j n_j^2 = 1.0$. The excess of supporting electrolyte accomplished, as usual, the suppression of the ζ-potential to negligible values, minimal tranference numbers t_j, and the virtual constancy of the activity coefficients of all reacting species S_j, thereby making the substitution of c_j for a_j possible.

Electrolyte solutions.—Both the toluquinone and the toluhydroquinone used were obtained from Eastman Kodak "practical grade" reagents. The toluquinone was purified by sublimation under atmospheric pressure and the sublimate collected as canary-yellow needles (mp 68.0°C). The toluhydroquinone, however, required repeated recrystallization from benzene and had to be subsequently twice sublimed in vacuo before snow-white crystals could be obtained (mp 126.5°C). All other reagents used in the electrolyte solutions were of C.P. quality and were used without further purification. Triply distilled water served as the solvent. The toluquinone and toluhydroquinone concentrations varied from 10^{-2} to 10^{-4} molar.

Because of the known vulnerability of aqueous solutions of toluquinhydrone to photodecomposition (7) the toluquinone and toluhydroquinone were dissolved in the electrolyte immediately before the start of each experiment. No decomposition could be detected within a 6-hr period, provided that the solutions were kept free of dissolved oxygen. Purified argon was, therefore, bubbled through the electrolyte at the start of each series and also, intermittently, between individual measurements within a series of determinations of the overpotential. This procedure insured sufficient stability during the 2-3 hr normally required for establishing the anodic and cathodic current density-potential relation at a given concentration.

Reference electrodes.—The values of all electrode potentials ϵ are referred to the SHE and were measured against a Ag/AgCl/KCl(1M) electrode ($\epsilon_0 = +0.2387$ V). Highly stable reference electrodes were prepared by the electrolytic formation of AgCl on thermally reduced spheres ($r \sim 0.2$ cm) of Ag_2O (8) attached to small Pt spirals. The scatter of potential differences among these electrodes never exceeded 0.05 mV.

Electrolysis cell.—A Pyrex cell as shown in Fig. 1 was used in all the polarization measurements described in this paper. The working electrode, a smooth Pt wire ($r \sim 0.25$ mm), was sealed into a glass tube leaving 2.55 cm exposed to the electrolyte solution, and was located along the axis of a cylindrical Pt counter-electrode through which a small hole had been drilled to accommodate the Haber-Luggin capillary of the

* Electrochemical Society Active Member.
Key words: toluquinhydrone electrode, reaction mechanism, exchange current densities, electrochemical reaction order.